

Catalysis Science & Technology

Accepted Manuscript



This is an *Accepted Manuscript*, which has been through the Royal Society of Chemistry peer review process and has been accepted for publication.

Accepted Manuscripts are published online shortly after acceptance, before technical editing, formatting and proof reading. Using this free service, authors can make their results available to the community, in citable form, before we publish the edited article. We will replace this *Accepted Manuscript* with the edited and formatted *Advance Article* as soon as it is available.

You can find more information about *Accepted Manuscripts* in the [Information for Authors](#).

Please note that technical editing may introduce minor changes to the text and/or graphics, which may alter content. The journal's standard [Terms & Conditions](#) and the [Ethical guidelines](#) still apply. In no event shall the Royal Society of Chemistry be held responsible for any errors or omissions in this *Accepted Manuscript* or any consequences arising from the use of any information it contains.



Journal Name

ARTICLE

Photocatalytic Reduction of CO₂ Coupling with Alcohol Selective Oxidation under Ambient Conditions

Liuji Wang^{a,b}, Xiaoliang Zhang^{a,b,*}, Longhua Yang^a, Chao Wang^a, and Hongming Wang^{a,*}

Received 00th January 20xx,
Accepted 00th January 20xx

DOI: 10.1039/x0xx00000x

www.rsc.org/

A new method for the reduction of CO₂ to CH₃OH coupling with alcohol selective oxidation by photocatalytic method has been developed in the present paper. CO₂ as oxidant was reduced to methanol by photo-induced electrons. And aromatic alcohol was used as reductant to react with photo-generated holes, converting to aromatic aldehyde with high selectivity. The maximum conversion of aromatic alcohol to aldehyde is 91.7 % with selectivity of 98 %, and the highest yield of methanol is 358.7 μmol g⁻¹. This study would provide a valuable method not only for carbon dioxide conversion into fuel which could remission energy shortage, but also for selective oxidation of alcohol to produce aldehyde.

1. Introduction

The photocatalytic conversion of solar energy into nonpolluting and usable chemical energy keep a great interesting always. Since Fujishima and Honda et al. found the production of hydrogen and oxygen by photocatalyzing water slipping in 1972¹, photocatalysis in various systems have been investigated. Especially, Tooru et al had demonstrated photocatalytic synthesis formic acid, formaldehyde, methyl alcohol and methane from carbon dioxide over photosensitive semiconductor powders catalysts in water medium². Subsequently, many research efforts have been done to address photocatalytic reduction of CO₂. The photocatalytic reduction of CO₂ into organic small molecules also have been become a great intention in recent years³⁻⁵.

Being a cheap, stable, nontoxic, and environmentally friendly material, titania (TiO₂) is an idea semiconductor photocatalyst. As a versatile material, TiO₂ is extensively applied in various photocatalytic reactions. In the particular case of CO₂ photoreduction, one of the efficient photocatalysts is metal-doped titania⁶⁻⁹. Copper doping is the most efficient way to enhance selectivity towards CH₃OH production and formation of formic acid derivatives in the photoreduction of CO₂¹⁰. Silver doped crystalline titania (Ag-TiO₂) prepared by the sol-gel method has been reported recently for CO₂ reduction to CH₄ and CH₃OH as main products in the photocatalytic reduction of CO₂ in water solution.¹¹

In fact, the majority of these studies in the literatures are carried out in liquid H₂O as the reaction medium in photocatalyzing reduction of CO₂⁶⁻¹¹. It could be interesting to check other solvents that are more difficult to reduce than H₂O¹². In addition, alcohols also allow the presence of Brönsted acids, which could favour the thermodynamics of the reduction. It is possible that photocatalytic reduction of CO₂ coupled with alcohols selective oxidation in organic solvent would be more efficient than that in the water. Actually, only a few groups¹³ studied this kind of photocatalytic reaction in organic media.

The selective oxidation of alcohols to corresponding aldehydes, in particular benzyl alcohol to benzaldehyde conversion^{14,15}, is one of the most popular organic transformations and is of fundamental importance for laboratory and commercial processes. Since aromatic aldehydes are widely used in the fragrances, flavorings, pharmaceutical industries, plastic additives, and is also highly valuable for the perfume industry. Heterogeneous photocatalysis have also been used for performing alcohols selective oxidation. A number of studies have been reported on the selective catalyst oxidation of alcohol into aldehyde under O₂ using a series of photocatalysts¹⁶⁻¹⁹. Moreover, the facile preparation method using inexpensive transition metals with a more selective and environmentally friendly system for the catalytic oxidation of aromatic alcohols to the corresponding aldehydes is certainly more in demand.

Photocatalytic reduction of CO₂ into organic small molecules coupling with alcohols selective oxidation to aldehydes in organic solvent have a certain practical value and application prospect, and is challenging. This reaction, not only is able to convert carbon dioxide into fuel, but also is able to convert alcohol to aldehyde with high selectivity. However, to the best of our knowledge, there is no report on photocatalytic reduction of CO₂ into organic small molecules coupling with alcohols selective oxidation to aldehydes. In this paper, a

^a Institute for Advanced Study and College of Chemistry, Nanchang University, Xuehu Road 999, Nanchang City, 330031, China. Email: Hongmingwang@ncu.edu.cn

^b College of Chemistry and Chemical Engineering, Jiangxi Normal University, Ziyang Road 99, Nanchang City, 330022, China. Email: xlzhang@jxnu.edu.cn

† Footnotes relating to the title and/or authors should appear here. Electronic Supplementary Information (ESI) available: [details of any supplementary information available should be included here]. See DOI: 10.1039/x0xx00000x

series of inexpensive and facile preparation photocatalysts, Ag/TiO₂ nanocomposites were fabricated from conventional sol-gel together with photo assisted methods. These kinds of catalysts have been used to explore the photocatalytic activity of CO₂ reduction coupling with aromatic alcohol oxidation in organic solvent.

2. Experimental

2.1 The preparation of titanium dioxide nanoparticle.

TiO₂ nanoparticle was prepared by modified sol-gel method. In a typical synthesis procedure, a volume of 20 ml of tetrabutyl titanate was dissolved in 80 ml of anhydrous diethyl ether at room temperature, and then 24 ml of acetic acid was added. After stirring this solution for 30 min, 30 ml mixture solution of double deionized water and acetic acid with the ratio of 2:1 (by volume) was added dropwise to the precursor solution under vigorously stirring. And that, a great plenty of white precipitate were formed in the solution. Subsequently the mixture was stirring keeping for 2 hours. The suspension was aged under airtight condition at room temperature for 24 hours. After suction filtration, the xerogel was washed several times by deionized water to remove the residual acid, and then dried at the 100 °C temperature for one day. Finally, the samples were divided into several sections and calcined at 400-800 °C for 2 hours in a muffle furnace at 5 °C/minute heating rate from room to setting temperature. Then, the sample was grounded to power in an agate mortar.

2.2 Synthesis of Ag/TiO₂ composites

Ag/TiO₂ nanoparticles were produced by photodeposition method. By using above synthetic TiO₂ nanoparticles as support of catalyst, 1g TiO₂ was dispersed in oxalic acid aqueous solution and sonicated for 15 min, then a predetermined amount of AgNO₃ was added to the solution and stirring for 2 hours to form homogeneous solution. Then these solution was irradiated on ultraviolet lam (PHILIPS TUV 25 W G2578 bactericidal lamp) for 4 hours under stirring 500 rpm at room temperature. When its colour was changed from white to reddish brown, the suspension was centrifuged at 10000 rpm and washed several times with deionized water. The xerogel was transferred to electronic vacuum oven and dried overnight at 60 °C.

2.3 Catalysts characterization.

XRD measurements were performed on a D8 diffractometer from Bruker instruments (Cu K α radiation, $\lambda=0.15406$ nm) operated at 40kV and 25mA. The diffractograms were collected at 2θ range from 20 to 80° in steps of 0.02°/min with count time 20s at each point. The crystalline phase can be determined from integration intensities of anatase and rutile corresponding to (101), (110) and (120), respectively. The average crystalline sizes were determined according to the Debye-Scherrer equation using the full width half maximum data of each phase. The nanoparticles average crystalline sizes of TiO₂ were determined according to $2\theta=25.3^\circ$ (101) face. SEM morphology of the samples was carried out using a scanning electron microscope (Quanta 200F FEI). The

transmission electron microscopy (TEM) was performed with a JEM 2100F transmission electron microscope equipped with EDX operated voltage at 200 kV. The TEM samples were prepared by sonication the powders in absolute alcohol for 15 minutes and subsequently dispersion on carbon coated copper grids drying at room temperature. UV-Vis diffuse reflectance spectra (UV-Vis DSR) were recorded using a SHIMADU UV-2550 UV-vis spectrophotometer with an integrating sphere attachment for their diffuse reflectance in the range of 300-800nm and using BaSO₄ powder as reference. The photoluminescence (PL) spectrum was recorded using a Perkin-Elmer LS55 fluorescence spectrometer at room temperature. The nanocomposites were dispersed in carbon tetrachloride and excited using D light at wave length of 265 nm.

2.4 Photocatalytic reduction of CO₂ coupling with aromatic alcohol selective oxidation activity test.

The reactions of photocatalytic CO₂ reduction coupling with aromatic alcohol oxidation were carried out in a 70 ml homemade double-jacket quartz glass reactor. 0.5g catalyst was added to the photo-reactor, 30 ml anhydrous acetonitrile (purified by calcium hydroxide and distilled before using) and 1mmol aromatic alcohol (purified by distilled before using) was subsequently put into the reactor. After that, the reaction cell was evacuated to base pressure of 10 kPa for 15 minutes to remove resolution oxygen, afterward high-purity CO₂ was filled into the reactor 30 minutes at a flow rate of 15 ml per minute. To ensure remove trace amounts of oxygen fully, such operation was repeated three times. In order to remove a trace amount of H₂O and oxygen in gas, the CO₂ gas was purified through allochroic silica gel, asbestos and activated carbon before importing into the reactor, respectively. And then, a balloon was connected to the reactor keeping the reaction under 0.1Mpa pressure. Before irradiation the suspension was kept at 500 rpm stirring for 60 minutes to ensure the CO₂ adsorption and desorption equilibrium. The ultraviolet (UV) light (high pressure mercury lamp main wavelength is 365 nm) was irradiation from the box wall before the reactor 10 cm. The liquid products were analyzed by Gas Chromatograph (GC) with flame ionization detector (FID). In order to analyse qualitatively the gas products, The gas chromatography-mass spectrometer (GC-MS) (7890A-5975C Agilent Corporation equipped with a HP-5 capillary column (Hewlett-Packard, USA, 30 m \times 0.25 mm \times 0.25 mm)), also used to identify the component of product. And the liquid products were also characterized by a Bruker vance 400MHz spectrometer (NMR).

3. Results and Discussion

The experimental details and characterization of the catalysts were showed in experimental section and supporting information. Figure 1 and S1 present the nanoparticles microscopes of TiO₂ and Ag/TiO₂ nanocomposites. From these representative morphologies, it can be clearly seen that TiO₂ crystallite is very well and its surface is smooth. Moreover, the

SEM and TEM image in figure 1 shows silver nanoparticles anchored on the surface of TiO_2 nanoparticles, silver nanoparticles are homogeneous dispersion on the surface of TiO_2 , formation a series of Ag/TiO_2 nanocomposites.

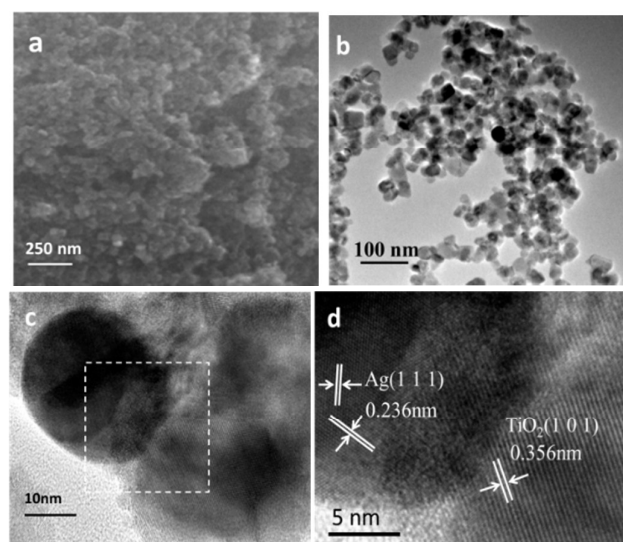


Figure 1. (a) SEM and (b) TEM image of ca. 3wt% Ag/TiO_2 nanoparticles. (c and d) HR-TEM image of ca. 3wt% Ag/TiO_2 nanoparticles.

To obtain more information of the catalysts, HR-TEM was used to observe these nanoparticles. Typical TEM micrographs of TiO_2 and Ag/TiO_2 nanoparticles catalysts are shown in Figure 1. From figure 1b, the relatively dark points are ascribed to Ag nanoparticles. The silver nanoparticles morphology is irregular spherical particles and have narrow size distribution, while the transparent region are assigned to TiO_2 in Figure 1b. Meanwhile, it was evident that average particle size of nanoparticles was 40-50nm, which was in good agreement with the XRD results calculated from Debye-Scherrer equation (figure S2). The HR-TEM was used to investigate the interfacial structures between Ag and TiO_2 (Figure 1c and 1d). In Figure 1c and 1d, the lattice fringes of Ag and TiO_2 showed surface-junction. The (111) lattice fringes of Ag nanoparticles was 0.236 nm, and the (101) lattice fringes of anatase was 0.356 nm. These results are agreement with the previous reports²⁰⁻²².

The photocatalytic reduction of CO_2 coupling with benzyl alcohol selective oxidation was carried out under ultraviolet light irradiation at 0.1 Mpa CO_2 pressure. The main liquid products were determined by GC (FID detector) (Figure S3). This result was also proved by ^1H NMR spectrum (Figure 2). When the reaction was carried out in CO_2 , the CO_2 was reduced to methanol, and benzaldehyde was the mainly product of the benzyl alcohol photocatalytic selective oxidation, along with a trace of benzoic acid and benzyl ether (Table 1). The highest conversion of benzyl alcohol is 10.3 % and 10.7 %, the maximum yield of methanol is 21.8 and 20.5 $\mu\text{mol g}^{-1}$ catalyzed by TiO_2 and ca. 1wt % Ag/TiO_2 after reacting 18 hours, respectively. However, as reacting in Ar gas

atmosphere, the highest conversion of benzyl alcohol is only 1.7 % and 1.9 %, and there is no methanol or other products to be observed, catalyzed by TiO_2 and ca. 3wt % Ag/TiO_2 catalysts, respectively. The blind test without catalyst (please see Table 1, Entry 19) shows that the conversion of benzyl alcohol is very low (0.75 %) and there is no methanol to be observed. These results verified that CO_2 is able to be reduced to methanol coupling with the selective oxidation of benzyl alcohol to benzaldehyde, and that the methanol is only produced from CO_2 , catalyzed by both TiO_2 and Ag/TiO_2 .

The effects of silver loading content on TiO_2 to the catalytic activity were evaluated as well. Compared to pure TiO_2 , the photocatalytic activity of ca. 2-6wt % Ag/TiO_2 nanocomposites exhibited a significantly increase (Table 1). Meanwhile, conversion of benzyl alcohol and the yield of the methanol both are drastically increased catalyzed by ca. 2-6wt % Ag/TiO_2 . It was found that the ca. 3wt % Ag/TiO_2 was optimum to achieve the highest conversion of benzyl alcohol (24.6 %) and maximum yield of methanol (40.9 $\mu\text{mol g}^{-1}$) after reacting 18 hours. When the silver loading content is less than 3wt %, the photocatalytic efficiency of catalyst is increased with silver loading content. It could be explained that the Ag nanoparticles deposited on the surface of TiO_2 can act as photo-induced carrier separation centers²³. Moreover, Schottky barrier was formatted between the silver and TiO_2 contact region, which improved the charges separation and enhanced the photocatalytic activity of TiO_2 ²⁴.

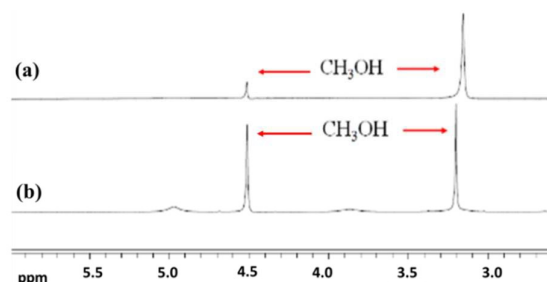


Figure 2. The ^1H NMR spectra of (a) the stand CH_3OH and (b) the product (MeOH) catalyzed by ca. 3wt% Ag/TiO_2 under 0.1 Mpa of CO_2 after irradiation for 48 hours.

However, when silver loading exceeds 3wt%, the photocatalytic activity rapidly decreases. The conversion of benzyl alcohol and yield of methanol are decreased from 24.6% to 14.9 % and from 40.9 to 14.9 $\mu\text{mol g}^{-1}$ with the increasing of silver loading content from 3 % to 9 %, respectively. It is maybe that exceeds silver nanoparticles cover the surface of TiO_2 activity sites that can absorb UV photon. Therefore, absorption photon capacity of the catalyst is reduced. And also, the exceeding silver nanoparticles can also act as recombination centers of electron and hole, which also results in the decreasing of the photocatalytic activity of Ag/TiO_2 nanocomposites. In fact, it has been reported that the probability for the hole capture increases by the large number of negating charged silver particles on the surface of TiO_2 at the high silver loading, which also increases the photo-induced electrons and holes recombination²⁵. These results are good

agreement with the photoluminescence (PL) spectra intensity of the photocatalysts showed in Figure S4. From figure S4, the PL intensities are decreased with increase of the Ag loading content when Ag loading content is less than 3wt %. The PL intensity signal is weaker, that photocatalytic efficiency is

higher. However, when the Ag loading content exceeds ca.4wt %, the PL intensities is increasing. It is indicated that excess silver deposited on the surface of TiO₂ can act as electron sinks to capture the photo-induced electrons and holes pairs.

Table 1. Production yields of the photocatalytic reduction of CO₂ coupling with benzyl alcohol selective oxidation under UV light irradiation on TiO₂ and Ag/TiO₂ catalysts.

Entry	Catalyst	RT ^b	Gas	CH ₃ OH	Benzyl alcohol	
				$\mu\text{mol g}^{-1}$	Con. [%]	Sel. [%]
1	TiO ₂	18	CO ₂	21.8	10.3	99
2	TiO ₂	18	Ar	—	1.7	99
3	P25	18	CO ₂	20.7	11.1	99
4	1%Ag/ TiO ₂	18	CO ₂	20.5	10.7	99
5	2%Ag/ TiO ₂	18	CO ₂	24.4	15.4	99
6	3%Ag/ TiO ₂	18	CO ₂	40.9	24.7	99
7	4%Ag/ TiO ₂	18	CO ₂	30.7	21.3	99
8	5%Ag/ TiO ₂	18	CO ₂	23.3	14.4	99
9	6%Ag/ TiO ₂	18	CO ₂	23.8	14.8	99
10	7%Ag/ TiO ₂	18	CO ₂	20.4	12.6	99
11	8%Ag/ TiO ₂	18	CO ₂	23.0	14.6	99
12	9%Ag/ TiO ₂	18	CO ₂	24.7	14.9	99
13	10%Ag/ TiO ₂	18	CO ₂	24.4	16.5	99
14	3%Ag/ TiO ₂	24	CO ₂	104.8	46.2	98
15	3%Ag/ TiO ₂	34	CO ₂	314.3	57.5	98
16	3%Ag/ TiO ₂	48	CO ₂	358.7	70.6	98
17	3%Ag/ TiO ₂	18	Ar	—	1.9	99
18 ^c	3%Ag/ TiO ₂	18	CO ₂	43.9	0.25	99
19	—	18	CO ₂	—	0.75	99
20 ^d	3%Ag/ TiO ₂	18	CO ₂	—	—	—

^aReaction condition: 40 ml CH₃CN, 1mmol benzyl alcohol; ^bReaction time; ^c Reaction condition: 40 ml benzyl alcohol; ^d Reaction condition: 40 ml CH₃CN, without benzyl alcohol.

Furthermore, the photocatalytic reduction of CO₂ to methanol coupled with various alcohols selectively oxidation have been performed over 3wt% Ag/TiO₂ under the same reaction conditions. The results are shown in Table 2. It is indicated that all catalyzing systems investigated were capable to convert CO₂ to methanol and convert the aromatic alcohols to corresponding aldehydes with different yield. The groups on the aromatic ring are effect on the reaction performing. The electron donating groups on the aromatic ring favors the methanol production and alcohols oxidation. For example, the methoxybenzyl alcohol can convert to p-anisaldehyde with conversions of 50.3% and 91.7%, and the yield of CH₃OH is 40.9 and 309.6 $\mu\text{mol g}^{-1}$ after reacting 18 and 48 hours, respectively. However, the drawing groups on the aromatic ring hold a low conversion. The conversion of p-nitrobenzaldehyde to nitrobenzyl alcohol is only 8.4% and 19.8% after reacting 18 and 48 hours, respectively. And the yield of

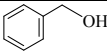
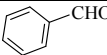
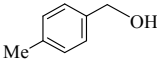
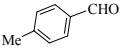
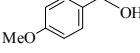
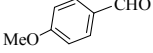
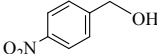
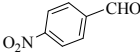
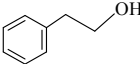
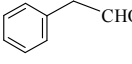
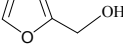
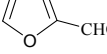


CH₃OH is low as well (13.6 and 79.5 $\mu\text{mol g}^{-1}$) under same reaction condition.

In order to know the stoichiometry of this reaction, the ratio of formation methanol and aldehyde have been calculated (the last column in table 2). The result shows that the ratio will be increased with prolongation of the reaction time. It can be explained that there are some intermediates to form (such as HCOOH, HCHO) in the initial phase. And at 48 hours, the highest ratio is 1:4 that is till smaller than the reaction stoichiometry (1:3). The first reason is that there are side-products, such as, H₂, CH₄, HCOOH, HCHO et al, was formed. For the second reason, with processing the reaction, the methanol also reacts with photo-generated holes to produce H₂ and CO₂. With the increasing of the concentration of methanol, this reaction is more and more fast. When the formation rate of methanol was most equated to the its' decomposition rate, production of methanol levels off.

Journal Name

ARTICLE

Table 2. Photocatalytic reduction of CO₂ to methanol coupling with alcohols oxidation with 3wt% Ag/TiO₂ catalyst

Entry	Substrate	Product	RT ^b	Yield ^c	Con.[%] ^d	Sel.[%] ^e	ME/Aldehyde ^f
1			18	40.9	24.7	99	1/12
			48	358.7	70.56	98	1/4
2			18	50.4	32.7	99	1/13
			48	219.4	74.6	98	1/6
3			18	73.3	50.3	99	1/13
			48	309.6	91.7	98	1/6
4			18	13.6	8.4	99	1/12
			48	79.5	19.8	99	1/5
5			18	121.6	61.6	99	1/10
			48	325.4	88.4	98	1/5
6			18	26.3	15.7	99	1/12
			48	63.4	27.3	98	1/8
7			18	14.7	8.9	99	1/12
			48	54.3	20.4	99	1/7

^a Reaction conditions: alcohols (1mmol), 3wt%Ag/TiO₂, stirred in 40 ml CH₃CN, under 0.1 MPa CO₂ and ultraviolet light (main wavelength of 365 nm) irradiation; ^bRT: reaction time; ^cunit: [μmol g⁻¹]; ^dconversion, of alcohol; ^eselectivity of benzaldehyd; ^f the ratio of formation methanol and aldehyde.

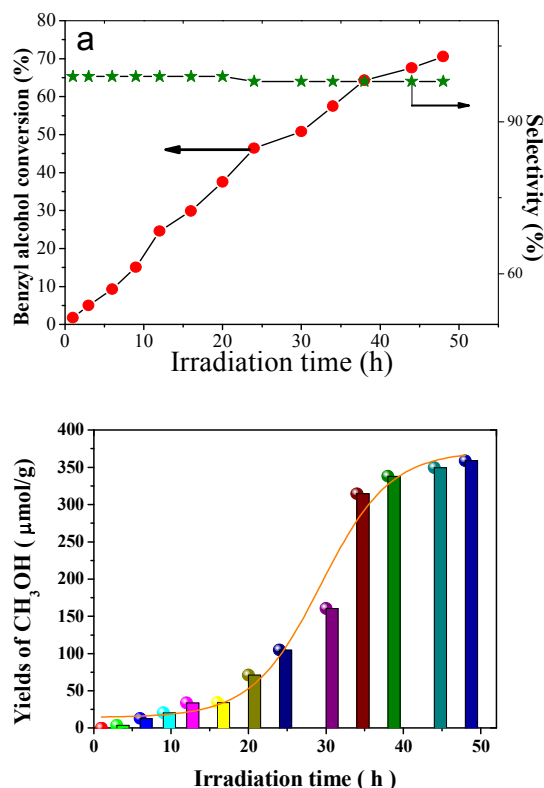


Figure 3. (a) The effect of irradiation time on conversion of benzyl alcohol and selectivity of benzaldehyde. (b) The yields of methanol production (unit: $\mu\text{mol g}^{-1}$) as function of irradiation time. (Reaction condition: 30 ml CH_3CN , 1 mmol benzyl alcohol 50 mg catalyst.).

The effect of irradiation time on photocatalytic reduction of CO_2 and benzyl alcohol conversion was investigated over a period of 1–48 hours on ca. 3 wt % Ag/TiO_2 nanocomposites catalysts (figure 3). With the increase of irradiation time, the conversion is clearly increased. However, the selectivity is slightly decrease due to by-products emerged in reaction system. The methanol yield is increased with the extension of irradiation time (Figure 3b). When the photoirradiation time is less than 18 hours, the increasing of yield is lowly. But when photoirradiation time is larger than 18 hours, the yield is obviously improving. After the photoirradiation time reaches to 45 hours, the yield of methanol is $344.6 \mu\text{mol g}^{-1}$ (figure 3b), and the conversion of benzyl alcohol is 70.6% with 98% selectivity of benzaldehyde.

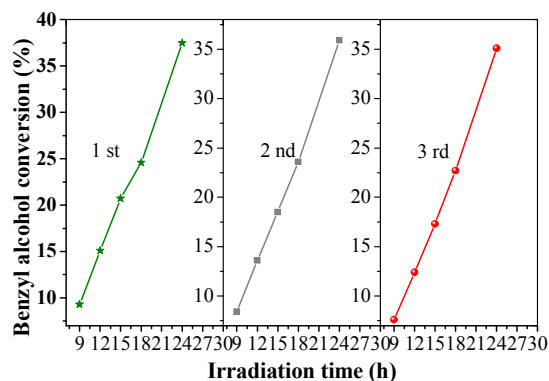
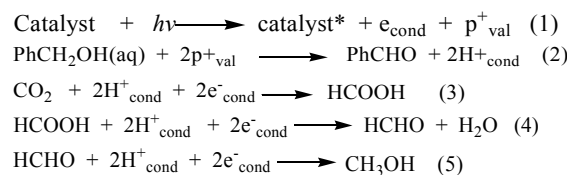


Figure 4. Photocatalytic reduction of CO_2 to methanol coupling with alcohols oxidation with 3 wt% Ag/TiO_2 catalyst in three cycles run.

In order to test the stability of Ag/TiO_2 nanoparticles catalyst, the used catalysts were recovered by centrifuged and thoroughly washed with anhydrous acetonitrile. The photocatalyst was recycled up to three times. As shown in Figure 4, its photocatalytic activity was only slightly deteriorated after three consecutive photocatalytic experiments. It can account for less silver nanoparticles leach and aggregation after the test, leading to the photocatalytic efficiency decrease weakly after three run times. The result showed that the photocatalyst was stable under repeated application with a constant conversion of benzyl alcohol to benzaldehyde.

To understand the reaction mechanism of CO_2 to methanol coupling with alcohols oxidation, the proposed mechanism for photocatalytic reduction of CO_2 to methanol coupling with alcohols oxidation is as follows:



Photogenerated holes in the VB of semiconductor oxidize alcohol to aldehyde and release H^+ (equation (2)), and photogenerated electrons in CB reduce carbon dioxide by sequence of reaction to produce HCOOH , HCHO and CH_3OH (equation (3), (2) and (5)).

4. Conclusions

The photocatalytic reduction of CO_2 coupling with alcohols selective oxidation was catalyzed by Ag/TiO_2

nanocomposites under UV light irradiation at room temperature and ambient pressure. CO₂ as oxidant was reduced to methanol by photo-induced electrons acted. And aromatic alcohol was used as reductant to react with photo-generated holes, converting to aromatic aldehyde with high selectivity. The optimal catalyst was ca.3wt % Ag/TiO₂ nanoparticles. The maximum conversion of aromatic alcohol to aldehyde is 91.7 % with selectivity of 98 %, and the highest yield of methanol is 358.7 μmol g⁻¹ under irradiation for 48 hours. Our findings may help to design more active photocatalysis system for the reduction of carbon dioxide and to open an environment-friendly strategy for the alcohol selective oxidation based on photocatalysis.

Acknowledgements

The support of the National Natural Science Foundation of China (21363014, 21106059 and 21103082) is gratefully acknowledged. This work was also supported by Natural Science Foundation of Jiangxi Province of China (Grant No. 20142BCB23003 and 20143ACB21021)

Notes and references

- 1 A. Fujishima, K. Honda, *Nature*, 1972, 238, 37-38.
- 2 T. Inoue, A. Fujishima, S. Konishi, K. Honda, *Nature*, 1979, 277, 637-638.
- 3 (a) S. N. Habisreutinger, L. Schmidt-Mende, J. K. Stolarczyk, *Angew. Chem. Int. Ed.* 2013, 52, 7372-7408. (b) X. Chen, J. Wang, C. Huang, S. Zhang, H. Zhang, Z. Li, Z. Zou, *Catal. Sci. Technol.* 2015, 5, 1758-1763.
- 4 S. Sato, T. Arai, T. Morikawa, K. Uemura, T.M. Suzuki, H. Tanaka, T. Kajino, *J. Am. Chem. Soc.* 2011, 133, 15240-15243.
- 5 (a) J. Tripathy, K. Lee, P. Schmuki, *Angew. Chem. Int. Ed.* 2014, 53, 12605-12608. (b) J. Mao, T. Peng, X. Zhang, K. Li, L. Ye, L. Zan, *Catal. Sci. Technol.* 2013, 3, 1253-1260.
- 6 (a) X. Chen, L. Liu, P. Y. Yu, S. S. Mao, *Science*, 2011, 331, 746-749. (b) J. Tripathy, K. Lee, P. Schmuki, *Angew. Chem. Int. Ed.* 2014, 53, 12605-12608. (c) K. Varghese, M. Paulose, T. J. Latempa, C. A. Grimes, *Nano Lett.* 2009, 9, 731-737.
- 7 (a) Q. Kang, T. Wang, P. Li, L. Liu, K. Chang, M. Li, J. Ye, *Angew. Chem. Int. Ed.* 2015, 54, 841-845. (b) C. Wang, R. L. Thompson, J. Baltrus, C. Matranga, *J. Phys. Chem. Lett.*, 2010, 1, 48. (c) M. Xing, F. Shen, B. Qiu, J. Zhang, *Science Reports*, 2014, 4, 6341. (d) Y. Yang, T. Zhang, L. Le, X. Ruan, P. Fang, C. Pan, R. Xiong, J. Shi, J. Wei, *Science Reports*, 2014, 4, 7045.
- 8 (a) J. Pan, X. Wu, L. Wang, G. Liu, G. Q. Lu and H.-M. Cheng, *Chem. Commun.*, 2011, 47, 8361. (b) L.-L. Tan, S.-P. Chai, A. R. Mohamed, *ChemSusChem* 2012, 5, 1868-1882. (c) L. Liu, C. Zhao, D. Pitts, H. Zhao, Y. Li, *Catal. Sci. Technol.*, 2014, 4, 1539-1546.
- 9 (a) H. Li, X. Zhang, D. R. MacFarlane, *Adv. Energy Mater.* 2015, 5, 1401077. (b) Y. T. Liang, B. K. Vijayan, K. A. Gray, M. C. Hersam, *Nano Lett.*, 2011, 11, 2865.
- 10 (a) M. Murdoch, G. I. N. Waterhouse, M. A. Nadeem, J. B. Metson, M. A. Keane, R. F. Howe, J. Liorca, H. Idriss, *Nature chemistry*, 2011, 3, 489-492. (b) Y. Li, W.-N. Wang, Z. Zhan, M.-H. Woo, C.-Y. Wu, P. Biswas, *Appl. Catal. B: Environ*, 2010, 100, 386.
- 11 (a) L. Li, J. Yan, T. Wang, Z.-J. Zhao, J. Zhang, J. Gong, N. Guan, *Nat. Commun.* 2015, 6, 5881. (b) S. Krejčíková, L. Matějová, K. Kočí, L. Obalová, Z. Matěj, L. Čapek, O. Šolcová, *Appl. Catal. B: Environ*, 2012, 111-112, 119.
- 12 Dhakshinamoorthy, S. Navalon, A. Corma, H. Garcia, *Energy Environ. Sci.* 2012, 5, 9217-9233.
- 13 V. Puga, A. Forneli, H. García, A. Corma, *Adv. Funct. Mater.* 2014, 24, 241-248.
- 14 T. Yokoyama, T. Setoyama, N. Fujita, M. Nakajima, T. Maki, K. Fujii, *Appl. Catal. A: General*, 1992, 88, 149.
- 15 S. Higashimoto, N. Kitao, N. Yoshida, T. Sakura, M. Azuma, H. Ohue, Y. Sakata, *Journal of Catalysis*, 2009, 266, 279-285.
- 16 X. Lang, W. Ma, C. Chen, H. Ji, J. Zhao, *Acc. Chem Res.* 2014, 47, 355-363.
- 17 (a) S. Liang, L. Wen, S. Lin, J. Bi, P. Feng, X. Fu, L. Wu, *Angew. Chem. Int. Ed.* 2014, 53, 2951-2955. (b) W. Chang, C. Sun, X. Pang, H. Sheng, Y. Li, H. Ji, W. Song, C. Chen, W. Ma, J. Zhao, *Angew. Chem. Int. Ed.* 2015, 54, 2052-2056.
- 18 A. Tanaka, K. Hashimoto, H. Kominami, *J. Am. Chem. Soc.* 2012, 134, 14526-14533.
- 19 S. Higashimoto, N. Suetsugu, M. Azuma, H. Ohue, Y. Sakata, *J. Catal.* 2010, 274, 76-83.
- 20 D. Wang, Y. Duan, Q. Luo, X. Li, J. An, L. Bao, L. Shi, *J. Mater. Chem.* 2012, 22, 4847-4854.
- 21 Z. Chen, L. Fang, W. Dong, F. Zheng, M. Shen, J. Wang, *J. Mater. Chem. A*, 2014, 2, 824-832.
- 22 Y. Li, H. Zhang, Z. Guo, J. Han, X. Zhao, Q. Zhao, S. Kim, *Langmuir*, 2008, 24, 8351-8357.
- 23 J. M. Herrmann, J. Disdier, P. Pichat, *J. Phys. Chem.*, 1986, 90, 6028-6034.
- 24 Y. Ji, B. Wang, Y. Luo, *J. Phys. Chem. C* 2014, 118, 21457-21462.
- 25 D. Tomova, L. Bilyarska, A. Eliyas, L. Petrov, *Appl. Catal. A: General*, 2006, 63, 266-271.

